POPULATION STUDIES IN GROUPS AND CLUSTERS OF GALAXIES. IV. COMPARISON OF THE LUMINOSITY FUNCTIONS AND MORPHOLOGICAL-TYPE DISTRIBUTIONS IN SEVEN NEARBY GROUPS

HENRY C. FERGUSON[1]
Henry Rowland Department of Physics and Astronomy, Center for Astrophysical Sciences, The Johns Hopkins University, Baltimore, Maryland 21218

ALLAN SANDAGE
The Observatories of the Carnegie Institution of Washington, 813 Santa Barbara St., Pasadena, California 91101
and
Henry Rowland Department of Physics and Astronomy, Center for Astrophysical Sciences, The Johns Hopkins University, Baltimore, Maryland 21218
and
Space Telescope Science Institute, 3700 San Martin Drive, Baltimore, Maryland 21218
Received 10 August 1990; revised 29 October 1990

ABSTRACT

Luminosity functions and morphological type fractions are examined in seven nearby groups of galaxies (Leo, Dorado, NGC 1400, NGC 5044, Antlia, Fornax, and Virgo). The groups are found to be similar in their fractions of early and late-type galaxies, consistent with the Dressler morphology–density relation and their similar mean densities. However, the dwarf-to-giant ratio *for early type galaxies* varies significantly with richness. The Virgo Cluster has ~ 5 times as many dwarfs per giant as the poorest groups (Leo, Dorado, and NGC 1400). In addition, the early type dwarf-to-giant ratio increases monotonically with the richness of the groups, and is possibly correlated with velocity dispersion. There is no evidence for radial gradients in the dwarf-to-giant ratio in the Antlia, Fornax, and Virgo Clusters. The composite giant + dwarf luminosity functions are not well fit by a Schechter function, but are best approximated by a bounded function (e.g., a Gaussian) for the giants, and a Schechter function with a faint end slope $\alpha \sim -1.3$ for the dwarfs. The difference between the flat slopes $\alpha \sim -1$ generally found for field and group samples, and the steeper $\alpha \sim -1.25$ generally found for clusters is reproduced in our sample when we restrict the data to galaxies brighter than $M_{B_T} = -16$. However, the very faint end $-12.5 \geqslant M_{B_T} \geqslant -16$ slope of the luminosity function in the poor groups is at least as steep as that in the Virgo Cluster. The conclusions are (1) although the *shapes* of the individual dwarf and giant luminosity functions remain the same, the ratio of the numbers of dwarfs to giants changes with environment; (2) this difference in the mixing ratio for the total luminosity function produces an artificial flattening at the faint end of the total function in those environments where the dwarf-to-giant ratio is low, such as in the field; and (3) it is likely that the faint end slope of the *dwarf* luminosity function is identical at $\alpha \sim -1.3$ in all environments.

1. INTRODUCTION

Knowledge of the luminosity function of galaxies is important for understanding the origin and evolution of structure in the universe and is essential if galaxies are to be used as probes of the geometry of the universe. Following Abell (1975), an assumption that is useful for some purposes is that the number of galaxies per unit luminosity in a given volume follows a universal law, that can parametrized following Schechter (1976) as

$$\phi(L)dL = \phi^*(L/L^*)^{\alpha} e^{-(L/L^*)} dL/L^*. \quad (1)$$

In the last two decades, the Schechter luminosity function with the parameters $M^*_{B_T} = -21$ and $\alpha = -1.25$ (for $H_0 = 50$ km s^{-1} Mpc^{-1}) has been shown to be a good fit to the observed distributions that are summed over all types (e.g., Schechter 1976; Felten 1977). However, it is likely that insight into the evolution of galaxies can be gained by considering a more general function $\phi(L,T,\rho,\mu,t,\ldots)$, taking into account variations of the luminosity function with galaxy type T, local density of the environment ρ, galaxy surface-brightness μ, the epoch t at which the galaxies are observed, and perhaps other parameters not yet uncovered.

Indications that such parameters are important come from the observed variations in the luminosity function from cluster to cluster (e.g., Oemler 1974; Dressler 1978), between clusters and loose groups (Turner & Gott 1976; Binggeli *et al.* 1988), and between clusters and the field (Kirshner *et al.* 1979; Tammann *et al.* 1979; Davis & Huchra 1982; Choloniewski 1986; Ellis 1983; Shanks *et al.* 1984; Phillipps & Shanks 1987). The latter studies tend to favor a flatter faint end ($\alpha \sim 1.0$) in regions of low density.

The Las Campanas Virgo Cluster survey (Binggeli *et al.* 1985) resulted in the first extensive investigation of $\phi(L,T)$ over a wide range of luminosities. It also provided some information on $\phi(L,T,\mu)$ (Sandage *et al.* 1985; hereafter referred to as SBT85). Investigations into the bivariate luminosity function $\phi(L,\mu)$ have been made by Choloniewski (1985) for E and S0 galaxies in the field, and by Phillipps & Disney (1986) for spirals in the Virgo cluster. A number of investigations of $\phi(L,\rho)$ (Binggeli 1987; Binggeli *et al.* 1988) and $\phi(L,t)$ (Spinrad 1986; Spinrad & Djorgovski 1987; Yee & Green 1987; Yoshii & Takahara 1988; Tyson 1988) have been carried out, with differing amounts of morphological resolution. However, the type-dependent luminosity functions for galaxies in clusters other than Virgo are poorly known. Thompson & Gregory (1980) computed LFs separately for ellipticals, spirals, and S0 galaxies in the Coma Cluster. They used these individual luminosity functions in varying proportions to construct synthetic LFs for various

[1] Present address: Institute of Astronomy, The Observatories, Madingley Road, Cambridge CB3 OH4, England.

 0004-6256/91/030765-18$00.90

mixtures of morphological types, and found that they were able to produce a scatter in α and M^* similar to the cluster-to-cluster variation reported by Dressler (1978). Dressler (1980) compared the LFs of S0 and Sp + Irr galaxies in high- and low-density regions of rich clusters, and found no evidence for a density-dependent effect. Type specific luminosity functions for galaxies in the *Revised Shapley–Ames Catalog* (RSA) (Tammann *et al.* 1979; Kraan-Korteweg *et al.* 1984) are similar to those found for the Virgo Cluster. However, quantitative comparison has not been performed and is complicated by the different completeness limits of the two surveys. The luminosity distributions constructed from the RSA reach only to $M_{B_T} \sim -18$, about where the LFs start to turn over for the high-surface-brightness galaxies, whereas the Virgo Cluster survey goes much fainter. Furthermore, the RSA is not a good list to use to obtain a "typical" field sample because it contains galaxies from both high- and low-density regions in proportions biased by the structure of the local supercluster. The results of these and other investigations have been reviewed by Binggeli *et al.* (1988; hereafter referred to as BST88).

Because of the difficulty of finding and estimating the distances to faint galaxies in the field, the luminosity function fainter than $M_{B_T} = -16$ has only recently begun to be explored. Fundamental changes in the observed properties of galaxies occur at this absolute magnitude. Brighter early type E and S0 galaxies typically have high-surface brightness and profiles that fall off roughly as $\exp(r^{1/4})$. The fainter dwarf elliptical and S0 galaxies are diffuse, low-surface-brightness objects with profiles that fall off more slowly. Dwarf spiral galaxies do not appear to exist. Their low-luminosity counterparts are the gas-rich dwarf irregular galaxies, which show no spiral features. The differences between giants and dwarfs, with the division at $M_{B_T} \sim -16$, may be due to (1) internal physical properties that govern the evolution of galaxies of different masses or (2) the influence of the external environment over the life of the galaxy. In either case, the study of the luminosity function and morphological mix of dwarf galaxies in different environments clearly offers promise for understanding the physics of galaxy evolution. Such studies also have two important implications for cosmology. First, it is not yet clear what contribution the dwarfs make to the total mass density of the universe. Knowledge of the formation and evolution of dwarfs is important here. Second, the clustering properties of dwarf galaxies as a function of morphology and luminosity offer important tests for the nature of the dark matter. Several recent models (Dekel & Silk 1986; White *et al.* 1987) based on the "Cold Dark Matter" (CDM) scenario suggest that low-luminosity galaxies are more smoothly distributed than giant galaxies. Whether or not such "bias" exists on large scales, recent simulations of cluster collapse in the presence of dark matter (West & Richstone 1988) show that segregation between less massive galaxies might be expected in present day clusters. These simulations assumed that 10% of the cluster mass is contained in galaxies, and 90% of the mass is contained in particles 10 times less massive than the galaxies (which the authors label "dark matter," but which may be equally accurately termed "dwarf galaxies"). After cluster collapse, the harmonic mean separation of the lighter particles is typically a factor of 5 larger than that of the heavier particles. The relevance of this to real clusters depends on what fraction of the dark halos remains "attached" to the galaxies.

A large number of observational studies aimed at determining the clustering properties of galaxies as a function of luminosity have been made (e.g., Sharp *et al.* 1978; Davis & Djorgovski 1985; Giovanelli *et al.* 1986; Bothun *et al.* 1986; Thuan *et al.* 1987; Phillipps & Shanks 1987; Tully 1988; White *et al.* 1988; Eder *et al.* 1989; Binggeli 1988; Binggeli *et al.* 1990; Salzer *et al.* 1990). The results have been contradictory. Some studies claim that low-luminosity galaxies are more smoothly distributed; others fail to detect significant spatial differences as a function of luminosity. In studies based on large samples of galaxies with 21 cm line velocities measured from Arecibo, Eder *et al.* find that the correlation function for dwarf galaxies is indistinguishable from that of galaxies in the CfA redshift survey, whereas Salzer *et al.* (1990) found a difference in the correlation function of low-luminosity galaxies at the level predicted by the models of White *et al.* (1987). In any event, the differences in clustering of the bright and faint galaxies are subtle, and are, of course, linked to the morphology–density relation and the selection biases of the samples. For example, studies that show that *late-type* low-luminosity galaxies, i.e. dwarf irregulars, are less clustered than bright galaxies, beg the issue of whether the late-type dwarf galaxies that might have been found in clusters have been preferentially converted to early type galaxies.

The variations in the luminosity function with environment due to *initial conditions* (bias) are difficult to disentangle from the variations due to the effects of clusters on their own member galaxies. In this and the two papers to follow in this series, we use samples of galaxies in five nearby groups (Ferguson & Sandage 1990; hereafter referred to as Paper III), the Virgo Cluster (BST85), and the Fornax Cluster (Ferguson 1989; Paper II) to (1) study the variations in the luminosity function with environment, and (2) examine the clustering properties of dwarf galaxies. In the present paper, we compare the galaxy populations and luminosity functions in the different groups. In Paper V, the catalogs will be resampled by the local density to test if the luminosity function depends on local environment. Finally, in Paper VI, we will examine the morphology-density for dwarf galaxies.

The combined surveys of the Fornax and Virgo Clusters reported in previous papers comprised 93 du Pont plates, covering a total area of 24 Mpc^2. Fourteen additional plates, covering a total area of 12 Mpc^2, were obtained for the Leo, Dorado, NGC 1400, NGC 5044, and Antlia groups. Because the coverage of these groups is less complete and less homogeneous than for the Fornax and Virgo surveys, this part of the investigation is of a more exploratory nature than the preceding papers. Sources of error and selection effects that might affect the comparisons between the groups are discussed in Sec. 2. In Sec. 3, the morphological-type distributions of the different groups are compared to see if the ratio of early to late-type galaxies or dwarfs to giants varies from place to place. Correlations of these ratios with group properties (e.g., richness, mean density, central density, velocity dispersion) are discussed. In Sec. 4, we compare the differential luminosity functions of the different samples. Section 5 contains a summary of the conclusions.

2. COUNTING CONVENTIONS, SOURCES OF ERROR, AND SELECTION EFFECTS

We consider first the sources of error and biases that arise in the less homogeneous data sample from Paper III compared to the Fornax and Virgo surveys.

2.1 Uncertainties in the Absolute Magnitudes

The random uncertainty in the eye-estimated B magnitudes from Paper III is approximately 0.5 mag. Systematic errors due to zero-point offsets appear to be small ($\sim$0.1 mag), as found by a comparison of our eye-estimated magnitudes in these groups to published magnitudes for the bright galaxies. By comparison, the estimates of the distance moduli (relative to Virgo) for some of the groups (Leo, NGC 1400, and NGC 5044 in particular) are uncertain by up to 1 mag. The zero-point errors in absolute magnitudes, then, are dominated by the distance uncertainties rather than the uncertainties of the estimated apparent magnitudes.

A second uncertainty is the possibility that some of the groups are not physical associations but are projections of galaxies along the line of sight. We examined this possibility in Paper III and found no evidence for such projections. In any case, as long as the contamination by interlopers is limited to a few isolated field galaxies, the comparison of the luminosity functions will not be seriously affected.

The most significant uncertainty at the faint end of the luminosity function is in the completeness correction that must be applied to the raw survey catalogs; see Sec. 5 of Paper III for a discussion of the corrections and their uncertainties.

2.2 Uncertainties in Classification

In counting the galaxies in various morphological bins, we have followed the convention of previous papers of dividing intermediate types evenly into the two individual classes. For example, the E/S0s have been taken 1/2 into the E class and 1/2 into the S0 class. The one exception to this rule is galaxies that have classifications "dE or S," or "Im or S." Here, the galaxies are classified as *either* cluster member dwarfs *or* background (usually low-surface-brightness) spirals. We have therefore added 1/2 to the appropriate dwarf bins for these galaxies. Galaxies with intermediate types constitute 7% of the sample of likely cluster members in all the groups. Because we have applied this counting procedure consistently to all the groups, the procedure does not affect the comparison of the luminosity functions or morphological type distributions between the groups.

In addition to the Hubble classifications, we have also assigned membership classifications to indicate the likelihood, based on morphology, that a galaxy actually is a member of a group. The number of galaxies classified as "possible members" (membership class 3 of Table 3.1) varies from group to group and with position in the groups. On average, 31% of the sample is of membership class 3. The percentage increases as a function of magnitude. Brighter than $B_T = 18$, less than 25% of the sample is of membership class 3. An additional 20% of the sample (excluding the Virgo Cluster) down to the survey limit is of membership class 2, defined as "probable members." (The Virgo Cluster survey did not have a membership class corresponding to our class 2.) Considered by absolute magnitude, the membership uncertainties are slightly greater for the more distant NGC 5044 and Antlia groups. For galaxies brighter than $M_{B_T} = -15$, 27% of the galaxies in these two groups are of membership class 3, compared to 21% in the Fornax and Virgo clusters. Note that foreground contamination as well as background contamination may be more significant for these groups; their luminosity functions should therefore be regarded as less secure than for the nearer groups.

The proportion of galaxies in membership classes 2 and 3 that *are actually* members of the clusters is unknown. We have arbitrarily assigned a probability of 100% for class 1, 80% for class 2, and 25% for class 3 and have weighted the number counts of these galaxies accordingly. In principle, one could make a statistical correction from the bivariate luminosity function $\phi(L,\mu)$ for the giant galaxies, calculating the fraction of galaxies at a given surface brightness that could be background galaxies projected on the cluster. In practice, however, $\phi(L,\mu)$ is not well known, and we have rejected a large fraction of the low-surface-brightness background galaxies anyway, based on details of their morphology (e.g., spiral features) visible with the large plate scale of the Las Campanas material. We have applied the weights consistently for all the groups, hence the luminosity functions should be directly comparable, in spite of possible contamination by background galaxies or underweighting of cluster members.

Note that the weighting schemes just described produce nonintegral numbers of galaxies in the final luminosity distributions.

3. THE DISTRIBUTION OF MORPHOLOGICAL TYPES

3.1 Comparison of the Groups

As a first-order comparison of the groups in this section we avoid the completeness corrections and ignore the differences in spatial coverage for the groups. Our aim is to establish whether there are any gross variations between the groups and the Virgo Cluster that are statistically significant. We find, indeed, that there are. We proceed, then in the sections to follow, to test if the variations are real by applying completeness corrections to the raw data, and by examining possible selection effects.

Table 1 shows the distribution of morphological types in the seven groups. The first column lists the group name. The second shows the total number of galaxies in the catalogs down to the magnitude limit shown. No corrections for different survey limits have been applied in this table. No data for the NGC 5044 and the Antlia Groups are given where the catalogs are substantially incomplete. All the groups are affected by incompleteness if galaxies are included down to $M_{B_T} = -12.5$; however, all but the Antlia group are likely to be complete down to $M_{B_T} = -15.5$. Nonetheless, it is of interest to push the comparison to faint limits in spite of the incompleteness, because the completeness corrections for Leo, Dorado, Fornax, and Virgo are nearly the same down to $M_{B_T} = -12.5$ and, in any case, are small. The remaining columns in Table 1 show the percentage of the total galaxy population of various morphological types.

The most basic comparison to the Virgo Cluster is in the ratio of early to late-type galaxies (in Table 2), and in the ratio of dwarfs to giants (in Table 3). The numbers in parenthesis in these two tables give a guide to the significance of the difference between the ratio for the group and the ratio for Virgo. Because the true parent population is not known, we have assessed the significance from the binomial distribution, assuming that Virgo is the parent population. For example, from the Virgo Cluster we assign a probability $P = 0.903$ for drawing a dwarf from the sample of all early type galaxies brighter than $M_{B_T} = -12.5$. Thus for the Dorado sample of 23 early type galaxies, we expect to find $nP = 20.6 \pm 1.4$ dwarfs [where the uncertainty is $\sqrt{nP(1-P)}$]. Dorado has only 15.8 dwarfs to this magni-

TABLE 1. Distribution of morphological types.

A. Galaxies brighter than $M_{B_T} = -12.5$

Group	N	E	S0	dE	dE,N	dS0	Sa-Scd	Sd-Im	BCD	Other
Leo	29.3	10.9%	6.1%	30.0%	13.0%	3.4%	12.3%	18.1%	4.1%	2.0%
Dorado	37.3	8.0	10.7	22.3	13.7	6.4	9.7	24.1	3.2	1.9
NGC1400	70.1	8.4	11.0	28.2	36.5	4.7	4.3	5.4	0.6	1.0
Fornax	332.7	7.2	5.4	37.4	23.5	6.3	6.0	11.2	1.5	1.6
Virgo	1079.5	3.0	4.3	39.3	25.2	3.3	9.1	11.7	2.3	1.8

B. Galaxies brighter than $M_{B_T} = -13.5$

Group	N	E	S0	dE	dE,N	dS0	Sa-Scd	Sd-Im	BCD	Other
Leo	22.4	14.3%	8.0%	15.2%	13.4%	4.5%	16.1%	22.3%	5.4%	0.4%
Dorado	30.9	9.7	12.9	9.7	15.9	7.1	11.7	27.2	3.9	1.3
NGC1400	49.0	12.0	15.7	13.5	38.2	6.1	6.1	6.3	0.8	1.2
Fornax	258.2	9.1	7.0	27.3	26.8	7.6	7.8	11.5	1.9	0.9
Virgo	780.0	4.1	6.0	25.4	28.2	4.6	12.6	14.3	3.2	1.7

C. Galaxies brighter than $M_{B_T} = -14.5$

Group	N	E	S0	dE	dE,N	dS0	Sa-Scd	Sd-Im	BCD	Other
Leo	16.5	19.4%	10.9%	9.1%	7.9%	6.1%	21.8%	16.4%	7.3%	0.6%
Dorado	23.0	13.0	17.4	2.2	10.9	9.1	15.2	26.5	4.8	0.4
NGC1400	38.2	15.2	20.2	7.9	32.7	7.6	7.9	7.3	0.5	1.0
NGC5044	90.7	12.5	9.0	31.3	20.2	2.4	6.4	15.0	2.1	1.0
Fornax	173.4	12.2	10.3	12.5	27.3	8.9	11.6	13.7	2.6	0.9
Antlia	239.0	7.7	9.5	38.9	14.9	5.3	5.7	16.2	1.0	0.8
Virgo	578.5	5.5	8.1	16.1	26.9	5.9	17.0	15.1	3.7	1.7

D. Galaxies brighter than $M_{B_T} = -15.5$

Group	N	E	S0	dE	dE,N	dS0	Sa-Scd	Sd-Im	BCD	Other
Leo	12.0	20.8%	15.0%	8.3%	0.0%	0.0%	29.2%	18.3%	8.3%	0.0%
Dorado	16.3	14.1	23.3	0.0	0.0	9.2	21.5	28.8	3.7	0.0
NGC1400	28.0	18.6	27.5	1.8	30.4	6.8	10.7	4.3	0.0	0.0
NGC5044	52.3	21.6	15.5	9.9	17.6	4.0	11.1	16.4	3.1	0.4
Fornax	109.5	15.4	15.5	4.5	19.3	8.1	18.4	15.1	3.3	0.5
Antlia	154.3	11.7	14.6	14.2	19.0	7.8	8.8	21.6	1.6	0.5
Virgo	426.5	7.4	10.8	9.7	21.1	7.9	23.0	14.9	3.1	2.1

tude limit, a difference that is significant at the 3.4σ level. These levels of significance are similar to those found by applying $\sqrt{N}$ statistics to the number counts in each group. A better test of the significance of the differences between the groups and Virgo is given below.

In general, the morphological-type distributions in Table 2 are quite similar. The groups are generally richer in early type giants than the Virgo Cluster. However, this is simply a bias in the sample of groups since no spiral-rich aggregates were included in the survey. The groups are also similar in the ratio of early type (dE) to late-type (Im) dwarfs, with the Leo and Dorado Groups being perhaps deficient in dEs and dS0s relative to Ims, and the NGC 1400 Group being deficient in Ims.

The most significant difference between the groups and the Virgo Cluster is in the dwarf-to-giant ratio. The three poorest groups (Leo, Dorado, and NGC 1400) all have fewer early type dwarfs per giant than the Virgo Cluster (at the 3–4σ level depending on the sample). The difference is not due to differences in the completeness limits. For example, to recover the Virgo early type dwarf-to-giant ratio in the Dorado Group one would have to have missed 75% of the dEs and dS0s (30 galaxies) brighter than $M_{B_T} = -13.5$ ($B_T = 18.1$), an unlikely result considering the error estimates on the completeness corrections in Paper III. Alternatively, five of the seven galaxies classified as giants would have to be in fact dwarfs. The differences between the groups persist even when a bright magnitude cutoff of $M_{B_T} = -15.5$ is applied. The richer groups (NGC 5044, Antlia, and Fornax) have a larger dwarf fraction than the poorest ones, but still have fewer dwarfs per giant than the Virgo Cluster.

A better estimate of the significance of the differences in the early type dwarf-to-giant ratio (hereafter referred to as the EDGR, for the sake of brevity) is to assess the probability of finding the observed EDGR for the groups if we select samples of the same size from random positions in the Virgo Cluster. The calculation is made by finding the intrinsic variation in the EDGR within the Virgo Cluster and asking if it is large enough to explain the differences among the groups as simply due to sample selection. To carry out the calculations, we have selected 2000 postions at random in the Virgo Cluster and have computed the EDGR for the nearest N

TABLE 2. Ratios of early to late-type galaxies.

A. Galaxies Brighter than $M_{B_T} = -12.5$

	Leo	Dorado	NGC1400	NGC5044	Fornax	Antlia	Virgo
N	29.3	37.3	70.1	118.7	332.7	251.1	1079.5
dE+dS0+dE,N/Im	2.57	1.76 (3)	12.82		6.00		5.78
E+S0+dE+dS0+dE,N/Sp+Im	2.09	1.81	9.16		4.63		3.60
dS0/dE	0.11	0.29	0.17		0.17 (3)		0.08
dE,N/dE+dE,N+dS0	0.43	0.61	1.29		0.63		0.64

B. Galaxies Brighter than $M_{B_T} = -13.5$

	Leo	Dorado	NGC1400	NGC5044	Fornax	Antlia	Virgo
N	22.4	30.9	49.0	118.3	258.2	251.1	780.0
dE+dS0+dE,N/Im	1.48	1.20	9.13		5.35		4.07
E+S0+dE+dS0+dE,N/Sp+Im	1.44	1.43	6.87		4.03 (3)		2.54
dS0/dE	0.29	0.73	0.45		0.28		0.18
dE,N/dE+dE,N+dS0	0.88	1.63	2.83		0.98		1.11

C. Galaxies Brighter than $M_{B_T} = -14.5$

	Leo	Dorado	NGC1400	NGC5044	Fornax	Antlia	Virgo
N	16.5	23.0	38.2	90.7	173.4	239.0	578.5
dE+dS0+dE,N/Im	1.41	0.84	6.57	3.60	3.55		3.23
E+S0+dE+dS0+dE,N/Sp+Im	1.40	1.26	5.50	3.53	2.81		1.95
dS0/dE	0.67	4.20	0.97	0.08	0.71		0.37
dE,N/dE+dE,N+dS0	0.87	5.00	4.17	0.64 (3)	2.19		1.68
E/S0	1.78	0.75	0.75	1.38	1.18		0.68
E+S0/Sp	1.39	2.00	4.50 (3)	3.36 (3)	1.95 (3)		0.80

D. Galaxies Brighter than $M_{B_T} = -15.5$

	Leo	Dorado	NGC1400	NGC5044	Fornax	Antlia	Virgo
N	12.0	16.3	28.0	52.3	109.5	154.3	426.5
dE+dS0+dE,N/Im	0.45	0.32	9.08	1.92	2.12	1.90	2.60
E+S0+dE+dS0+dE,N/Sp+Im	0.93	0.93	5.67	2.49	1.88	2.21	1.50
dS0/dE	0.00	-	3.80	0.40	1.82	0.55	0.81
dE,N/dE+dE,N+dS0	0.00	-	17.00	1.77	4.31	1.34	2.17
E/S0	1.39	0.61	0.68	1.40	0.99	0.80	0.68
E+S0/Sp	1.23	1.74	4.30 (3)	3.34 (3)	1.69	2.99 (5)	0.79

TABLE 3. Ratios of dwarfs to giants.

A. Galaxies Brighter than $M_{B_T} = -12.5$

	Leo	Dorado	NGC1400	NGC5044	Fornax	Antlia	Virgo
N	29.3	37.3	70.1	118.7	332.7	251.1	1079.5
dE+dS0+dE,N/E+S0	2.72	2.26 (3)	3.58 (3)		5.33 (3)		9.31
Im/Sp	1.47	2.50	1.27		1.85		1.29
dE/E+S0	1.76	1.19 (3)	1.46 (4)		2.97 (3)		5.39
dE,N/E+S0	0.76	0.73 (3)	1.88		1.86 (3)		3.46
dS0/E+S0	0.20	0.34	0.24		0.50		0.45

B. Galaxies Brighter than $M_{B_T} = -13.5$

	Leo	Dorado	NGC1400	NGC5044	Fornax	Antlia	Virgo
N	22.4	30.9	49.0	118.3	258.2	251.1	780.0
dE+dS0+dE,N/E+S0	1.48	1.44 (3)	2.08 (3)		3.83		5.77
Im/Sp	1.39	2.33	1.03		1.48		1.14
dE/E+S0	0.68	0.43 (3)	0.49 (4)		1.69		2.53
dE,N/E+S0	0.60	0.70	1.37		1.67		2.80
dS0/E+S0	0.20	0.31	0.22		0.47		0.45

C. Galaxies Brighter than $M_{B_T} = -14.5$

	Leo	Dorado	NGC1400	NGC5044	Fornax	Antlia	Virgo
N	16.5	23.0	38.2	90.7	173.4	239.0	578.5
dE+dS0+dE,N/E+S0	0.76	0.73 (3)	1.36 (3)	2.51	2.16		3.61
Im/Sp	0.75	1.74	0.93	2.34	1.18		0.89
dE/E+S0	0.30	0.07	0.22 (3)	1.46	0.55 (3)		1.19
dE,N/E+S0	0.26	0.36	0.93	0.94	1.21		1.99
dS0/E+S0	0.20	0.30	0.21	0.11	0.39		0.44

D. Galaxies Brighter than $M_{B_T} = -15.5$

	Leo	Dorado	NGC1400	NGC5044	Fornax	Antlia	Virgo
N	12.0	16.3	28.0	52.3	109.5	154.3	426.5
dE+dS0+dE,N/E+S0	0.23	0.25 (3)	0.84	0.85 (3)	1.03 (3)	1.56	2.12
Im/Sp	0.63	1.34	0.40	1.48	0.82	2.46 (4)	0.65
dE/E+S0	0.23	0.00	0.04	0.27	0.14 (3)	0.54	0.53
dE,N/E+S0	0.00	0.00	0.66	0.47	0.62	0.72	1.16
dS0/E+S0	0.00	0.25	0.15	0.11	0.26	0.30	0.43

galaxies in the Virgo Cluster Catalog, where N is the number of galaxies in the group. Selecting 22 galaxies brighter than $M_{B_T} = -13.5$ each time, we find that we reproduce the Leo Group dE + dE,N + dS0/E + S0 ratio only 1.2% of the time, the Dorado group ratio (using 31 galaxies) 0.4% of the time, and the NGC 1400 group ratio (using 49 galaxies) 1.1% of the time. Therefore it is highly unlikely that the Virgo Cluster dwarf-to-giant ratio represents a universal quantity that applies to all galaxy aggregates.

In contrast to the early type galaxies, there are no significant variations in the dwarf-to-giant ratio in Table 3 for the late-type (spiral and irregular) galaxies. Variations in the combined dwarf-to-giant ratio (dE + dS0 + Im/E + S0 + Sp) are consequently only marginally significant.

3.2 Galaxy Morphology and the Properties of the Groups

3.2.1 Mean density

The morphology–density relation (Hubble & Humason 1931), has been extensively studied for galaxies brighter than $M_{B_T} \sim -17.5$ over six orders of magnitude in *local* galaxy density (e.g., Dressler 1980; Postman & Geller 1984). Being a local effect, the relation does not specifically predict global population differences *between* groups. The high-density cores of rich clusters typically have a high fraction of early type galaxies. However, the outer regions of rich clusters have densities that overlap those of less-dense groups of galaxies, and late-type galaxies that are members of the clusters tend to reside in these outer regions. Therefore, the morphology–density relation is diluted if considered as a function of the *mean* cluster density. Such an effect is presumably responsible for the scatter in the rich cluster populations shown by Dressler (1980; Fig. 2 and 3). For the groups considered here, the mean surface density of galaxies brighter than $M_{B_T} = -15$ spans only a factor of 2.7 in mean density. Hence, the similarity in the ratio of early to late-type galaxies observed for our sample is entirely consistent with the morphology–density relation. The implication is that the EDGR, which *does* vary from group to group, is probably *not* dependent on local density, but rather is related to some *global* property of the group.

3.2.2 Richness

The most obvious parameter that varies between the groups in the present survey is richness. The dwarf-to-giant ratio is plotted against the number of galaxies on the survey plates in each group in Fig. 1 for early types and Fig. 2 for all types. The dwarf-to-giant ratios are from the raw data, uncorrected for luminosity incompleteness. The richness is defined as the number of galaxies on the plates down to the magnitude cutoffs shown, uncorrected for incompleteness in spatial coverage. There is evidently a strong correlation with richness, even without the aforementioned corrections, in the sense that *poorer clusters have fewer dwarfs per giant galaxy*.

Consider now four possible selection effects that could produce the EDGR variation with richness in the sense observed.

(1) The surveys of some of the groups do not encompass all of the group volume. Paper III, Table 9 shows that the trend from the poorest to the richest groups is also a trend of increasing areal coverage (in Mpc^2). If the poorer groups are smaller, this is harmless because the incompleteness cannot destroy the correlations in Fig. 1, only make them steeper. The "true" abscissa values for the poor groups move more to the right while the richer groups remain closer to where they are. However, due to incomplete sampling, the number of galaxies on the plates may not reflect the true richnesses of the groups. The correlation with richness may

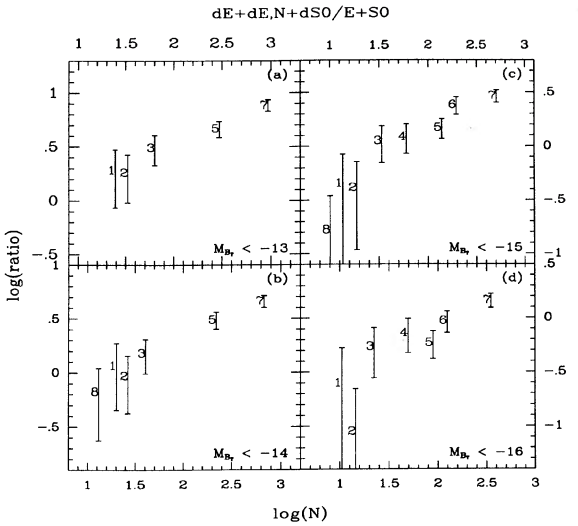

FIG. 1. Ratio of early type dwarfs to early type giants vs the the total number of galaxies down to the limiting magnitude shown. No completeness corrections have been applied. The numerator includes all dE, dE,N, and dS0 galaxies, and half the d:E, d:S0, and dS0/a galaxies. The denominator includes all E and S0 galaxies, half the S0/a galaxies, and half the d:E and d:S0 galaxies. The coding is: 1 = Leo, 2 = Dorado, 3 = NGC 1400, 4 = NGC 5044, 5 = Fornax, 6 = Antlia, and 7 = Virgo. The additional point (8) is taken from the nearby group sample of Kraan-Korteweg & Binggeli (1990) used to produce the luminosity functions for the "local field" in Binggeli *et al.* (1988). The richness for this particular data point is the total number of galaxies in the sample down to the magnitude limit shown, divided by the number of groups (7). The vertical position of the number marks the position of the datapoint.

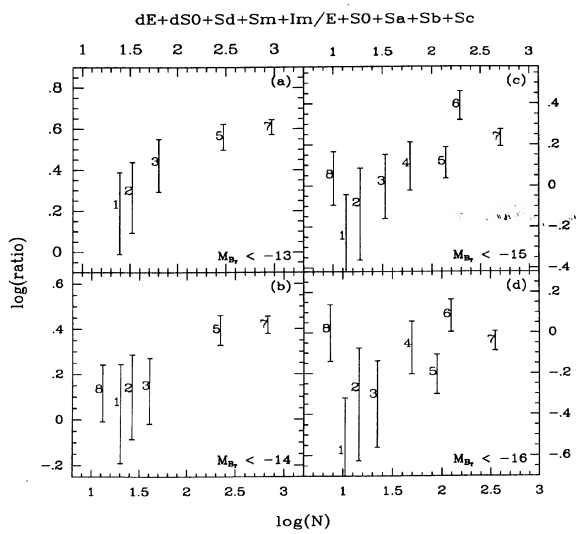

FIG. 2. The ratio of all dwarfs to all giants vs richness. Coding is the same as in Fig. 1.

not then be as strong if the corrections to the richnesses due to incomplete sampling are large. To estimate this effect, we have computed the number of galaxies that would be found within $5r_c$ of the cluster center from the density profiles shown in Paper III. The correlations are not substantially altered using the corrected richness values. (NGC 1400 becomes slightly poorer than Leo, otherwise the order of the richness is preserved.)

(2) Consider next the effect of radial gradients in the dwarf-to-giant ratio. In particular, *if* the EDGR were much lower in the centers of clusters than in their peripheries, *and* the poorest groups were surveyed to a smaller fraction of their true radii than the richest groups, *then* the poorest groups would appear to have the lowest EDGR. This cannot be a significant effect because (a) the poor groups have not been surveyed to a much smaller fraction of their scale radii than the rich ones (see Paper III, Table 11, and Fig. 15 and 16), and (b) there is no evidence for radial gradients in the EDGR in any of the groups (see Sec. *3.2.4* below).

(3) Because we have used the number of galaxies down to faint magnitude limits as a measure of richness, the ordinate and abscissa of Figs. 1 and 2 are correlated. For a fixed number of giant galaxies, these figures would show an apparent correlation with richness simply due to variations in the number of dwarfs. But, this is a minor effect, shown as follows. The correlation with richness is still strong for the groups in our sample if richness is defined *solely from the giants*. Indeed, Fig. 3 shows that the number of early type dwarfs increases significantly *faster* than the number of early type giants as one moves to the richer groups.

(4) It is important to note that the correlations here are based on galaxy *morphology*, not luminosity. Because the two parameters are not independent it is possible to separate faint cluster members from the background, but there is a substantial overlap in luminosity between the dwarfs and the giants. Figure 4 shows the ratio of faint to bright early type galaxies as a function of richness when no attempt is made to separate the giants and dwarfs by morphology. Panels (a),(b), and (d) show that the correlation still holds using luminosity separation alone. In contrast, panel (c) shows that the ratio of very faint ($-12.5 < M_{B_T} < -14.5$) to faint ($-14.5 < M_{B_T} < -12.5$) does not vary from group, indicating that slope at the very faint end of the luminosity function is not changing with richness.

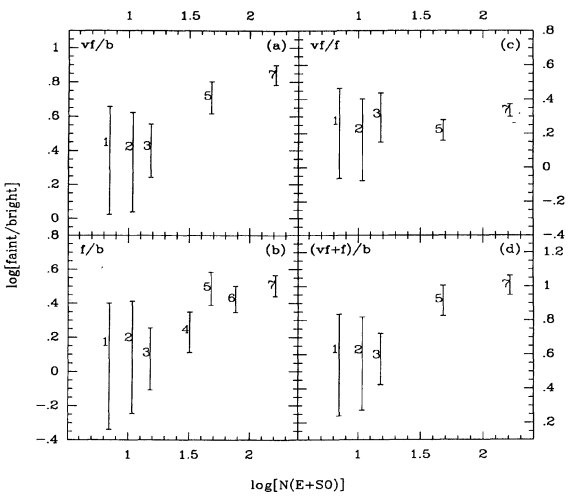

FIG. 4. The EDGR when galaxies are separated by luminosity alone, using no morphological criteria. Three samples of early type galaxies are defined: very faint (*vf*), with $-12.5 \geqslant M_{B_T} > -14.5$; faint (*f*), with $-14.5 \geqslant M_{B_T} > -16.5$; and bright (*b*), with $M_{B_T} \geqslant -17.5$. The different panels show the ratios of the numbers in the different samples vs richness as defined by the number in the bright sample. Panel (a) shows *vf*/*b*, (b) shows *f*/*b*, (c) shows *vf*/*f*, and (d) shows (*vf* + *f*)/*b*. Panel (c) indicates that the ratio of bright dwarfs to faint dwarfs does not vary from group to group, contrary to the trend in panels (a), (b), and (d). Coding is the same as in Fig. 1.

We will discuss the luminosity function in greater detail in Sec. 3. Note here, however, that the difference between the groups is still significant even at the brighter magnitude cutoffs, indicating, first, that uncertainties in the completeness corrections at faint magnitudes cannot account for the differences in the dwarf-to-giant ratio, and, second, that at least some of the variation from group to group must be due to changes in the numbers of *bright* dwarfs, in the region where they begin to overlap with the giants. A possible implication is that luminosity (or mass) may not be the only parameter that determines the morphology of an early type galaxy. Environment may also play a role. In particular, if the giants and dwarfs are drawn from the same universal distribution function of masses, then the variation in the dwarf-to-giant ratio must be explained by a richness-dependent transformation of (high-surface-brightness) giants into (low-surface-brightness) dwarfs. Alternatively, the formation properties of protoclusters may influence the distribution function of masses of the galaxies that form within them. Again, we face a decision between initial conditions at formation or later evolution due to environment.

Finally, richness, in the way we have defined it here, is not the true independent variable in this correlation. Instead it must be a proxy for another physically related parameter, such as the total mass of the group, its velocity dispersion, the galaxy density in the core of the cluster, or temperature and density of the intracluster medium (ICM).

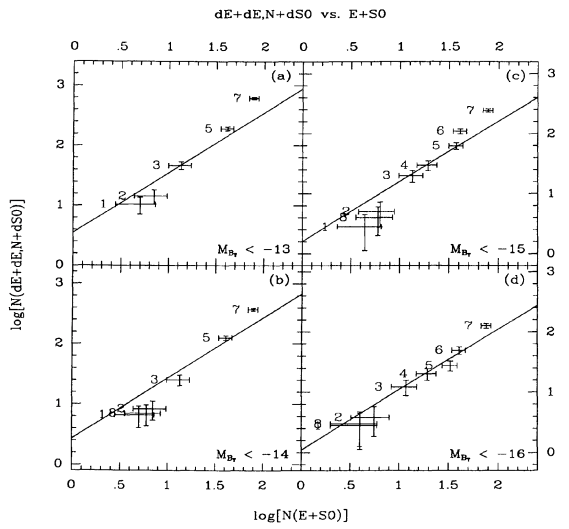

FIG. 3. The number of early type dwarfs vs the number of early type giants in the groups. The codings for the points are the same as in Fig. 1. The line shows the slope expected for a constant dwarf/giant ratio. The deviation of the data from this slope indicates that the dwarf population is increasing with richness faster than the giant population.

3.2.3 Structure and dynamics

The structural and dynamical properties of the groups were discussed in Paper III. The EDGR does not correlate well with either the core radii or the central densities of the groups shown there in Table 11. On the other hand, there is some evidence that it correlates with velocity dispersion. Figure 5, panel (a) shows the EDGR measured down to $M_{B_T} = -15.5$ plotted against the velocity dispersions of the groups, measured from all likely members in the Paper III catalogs. Panel (b) shows the correlation when just the velocities of the early type galaxies are used. Note that in both (a) and (b), the anomalous galaxy NGC 1400 has been removed from the NGC 1400 group sample, which otherwise would have a velocity dispersion several hundred kilometers per second higher. Even with this galaxy removed, the EDGR correlation with velocity dispersion is much weaker than with richness. However, this may be due to the small numbers of galaxies used to measure the velocity dispersions in some of the groups. Comparison of the velocity dispersions used here to others from the literature (Paper III, Table 13) showed a disparity of at least 100 km s^{-1} for the Dorado, NGC 1400, NGC 5044, and Antlia groups. The conclusion was that at least for the poor groups, the samples are not large enough to constrain the velocity dispersions reliably.

While direct comparison of the dynamical properties of the groups is not conclusive, the virial theorem can be used to extract dynamical information from the density profiles of the groups. A group in virial equilibrium with galaxies of average mass $\langle \mathcal{M}_G \rangle$ will have

$$N \langle \mathcal{M}_G \rangle \hat{v}^2 \sim (G \langle N \mathcal{M}_G \rangle^2 / R).$$

The average galaxy mass is therefore $\langle \mathcal{M}_G \rangle = R\hat{v}^2/NG$. If this average mass per galaxy does not vary from group to group then N/R varies as the square of the velocity dispersion. Panel (c) shows the correlation of the EDGR with the "observed" value of N/R if R is taken to be the core radius of the group. Panel (d) shows the results if the harmonic mean radius is used. The trends in (c) and (d) are similar to those in (a) and (b). Taken together, these trends suggest that the EDGR is correlated with the velocity dispersion of the group, but clearly the case must be strengthened using more velocities for these groups and a larger survey of additional groups.

3.2.4 Spatial variations in the dwarf-to-giant ratio

As mentioned above, the incomplete spatial coverage of the poorer groups could artificially produce a correlation of the dwarf-to-giant ratio with richness if the dwarf-to-giant ratio were correlated with position in the cluster. Mass segregation, and therefore dwarf-giant segregation, either from two-body relaxation over a Hubble time or from the dynamical relaxation in a cluster collapse time suggested by West & Richstone (1988) are expected to produce real physical gradients in the dwarf-to-giant ratio. Taking the number of galaxies in each group to be the number within $5r_c$, and assuming an average galaxy mass of $3\times10^{10}\ \mathcal{M}_\odot$, the values of two-body relaxation times τ_r computed from Eq. (8-72) of Binney & Tremaine (1987) are generally comparable to a Hubble time with uncertainties of at least an order of magnitude. The violent relaxation times from West & Richstone [1988, Eq. (13)] are about two orders of magnitude shorter. Radial gradients in the dwarf-to-giant ratio would be strong evidence that such mass segregation has occurred.

The EDGR is plotted as a function of radius in Figs. 6–8 for the Virgo, Fornax, and Antlia groups, respectively. There is no evidence for a radial gradient in these three clusters; the dwarf-to-giant ratios computed for different annuli do not differ significantly from the mean values found for each cluster, even though the mean ratios for each cluster are different. The EDGR is therefore a property of the cluster *as a whole*, not of the local environment, and in particular not

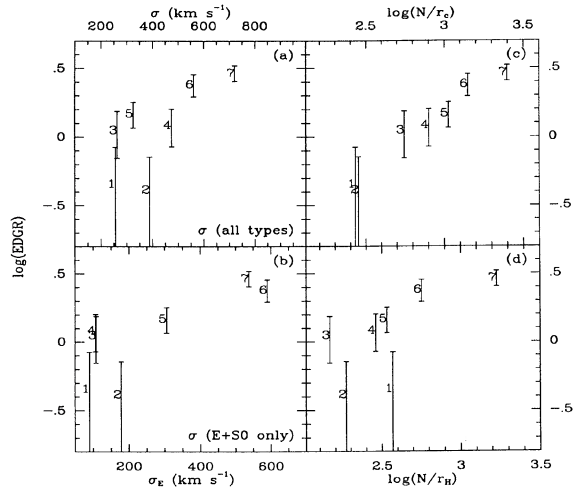

FIG. 5. The EDGR for galaxies brighter than $M_{B_T} = -15$ plotted against various measures of velocity dispersion. Panel (a) shows the EDGR vs the velocity dispersion as measured from galaxies of all types included in the catalogs in Paper III; (b) shows the EDGR vs the velocity dispersion of the *early* type galaxies only; (c) shows EDGR vs the quotient of the number of galaxies within $5r_c$ and the core radius based on the density profiles in Paper III; panel (d) is the same as panel (c) but uses harmonic mean radius r_H from Paper III, rather than r_c. Coding is the same as in Fig. 1.

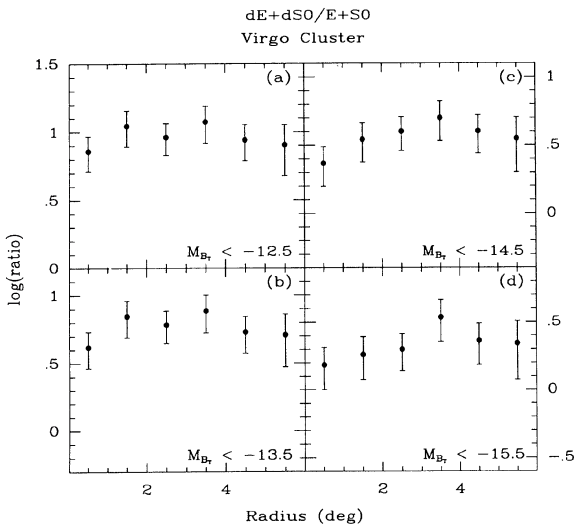

FIG. 6. The early type dwarf-to-giant ratio as a function of radial distance from the center of the Virgo Cluster. Ratios were computed in annuli of width 1°, centered on the nominal center of the cluster from Paper III.

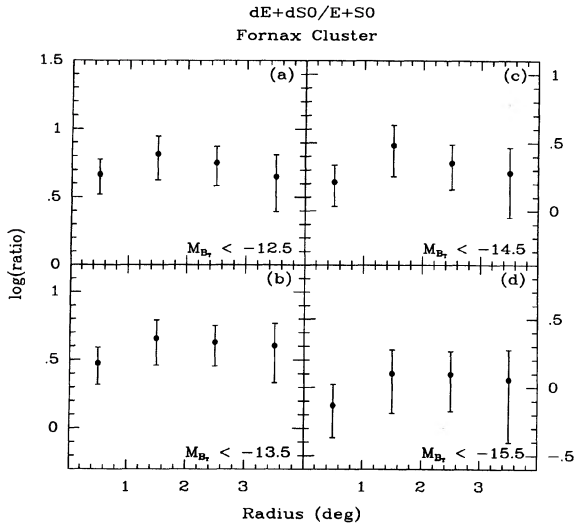

FIG. 7. The early type dwarf-to-giant ratio as a function of radial distance from the center of the Fornax Cluster. Ratios were computed in annuli of width 1°, centered on the nominal center of the cluster from Paper III.

of the radial coordinate. This is in marked contrast to the morphology–density relation, which is a function of *local* density, and is relatively insensitive to the other global properties of the clusters used to measure it. *The lack of a radial gradient is evidence that mass segregation has not occurred in these clusters.*

4. LUMINOSITY FUNCTIONS

The variations in the early type dwarf-to-giant ratio from group to group suggest that variations in the luminosity function must be present as a function of richness. Recall that the dwarfs have been identified on the basis of morphology rather than luminosity. The fact that the dwarf-to-giant ratio varies even when a bright magnitude cutoff is used suggests that the difference in the luminosity function is not simply a change in the faint-end slope. Rather, we shall show that it is a difference in the normalization of two separate luminosity functions, one for the bright galaxies (a near Gaussian) and one for faint galaxies (a near exponential). We begin by comparing the raw data, applying the Kolmogorov–Smirnov test to determine whether any of the differences between the groups are statistically significant.

As is customary, we then fit Schechter (1976) functions to the data to see if there are detectable differences in the α and M^* parameters. Note, however, that if the true luminosity function in the Virgo and Fornax clusters is, in fact, a combination of a bounded distribution for the luminous galaxies and a Schechter function for the dwarfs, it is unlikely that the Schechter function alone will be an adequate description for the total luminosity function as the dwarf-to-giant ratio changes.

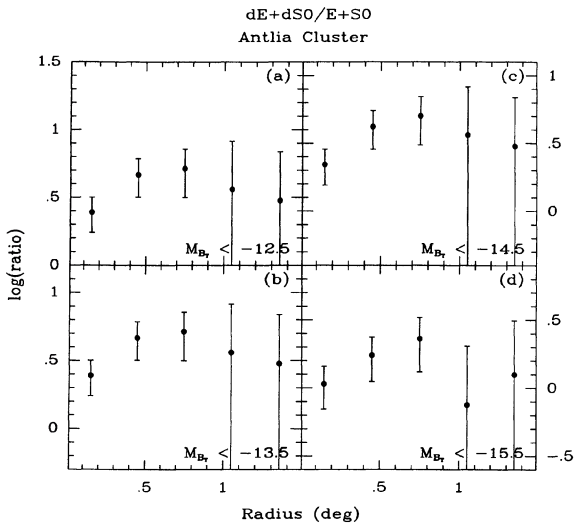

FIG. 8. The early type dwarf-to-giant ratio as a function of radial distance from the center of the Antlia Cluster. Ratios were computed in annuli of width 0.3°, centered on the nominal center of the cluster from Paper III.

4.1 Direct Comparisons

Luminosity functions for the individual groups are shown in Fig. 9, smoothed by 0.5 mag and broken into early and late-type giants and dwarfs. Comparison between the three poorest groups and the richer ones is hampered by small number statistics. Nonetheless, the ratio of the dwarf contribution to the total number of early type galaxies is clearly smaller in the groups than in Virgo, while the shape of the dE + dS0 luminosity function remains relatively constant. Panel (h) shows a composite of the Leo, Dorado, and NGC 1400 group luminosity functions, and Panel (i) combines the Virgo, Fornax, Antlia, and NGC 5044 Groups. The sense of the difference between panels (h) and (i) is that rich aggregates contain more dwarfs per giant than do poor aggregates, opposite to the sense expected from biased galaxy formation. Comparison of the two plots suggests that the break in the combined luminosity function for all types in the poor groups occurs at brighter magnitudes ($M_{B_T} \sim -21.5$) than in the rich groups ($M_{B_T} \sim -20$).

A comparison between the composite poor group and the Virgo Cluster is shown in Fig. 10. The plots are normalized by the total numbers of E and S0 galaxies. The difference in the dwarf-to-giant ratio is now readily apparent. The statistics are such that the luminosity functions shown for the early type giants are consistent with each other in shape, with a Gaussian dispersion of $\sigma \sim 2$ mag. A comparison of the shape of the combined dE + dE0 luminosity function is shown in Fig. 11, normalized by the total number of early type dwarfs brighter than $M_{B_T} = -13.5$. The luminosity-function shapes are nearly identical shown by inspection and by the detailed statistical analysis of the data (see below). In particular, the slopes of the luminosity functions at the faint end are the same to within the uncertainties. If there is any trend to a difference, it is that the group luminosity function is steeper than that for Virgo Cluster fainter than $M_{B_T} \sim -15$.

A composite "rich" group has also been formed as the sum of the NGC 5044, Antlia, and Fornax Groups. The comparison to the Virgo Cluster is shown in Fig. 12, once again normalized by the total number of early type giants. The shape of the luminosity function for the E and S0 galaxies is strikingly similar in the two samples. The composite rich group has marginally fewer dwarfs per giant than the

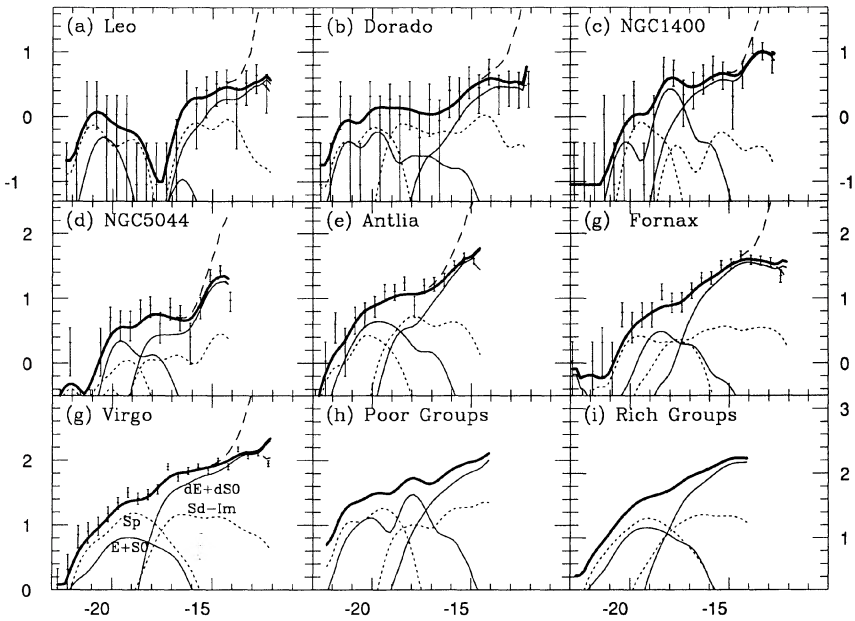

FIG. 9. Luminosity functions for the individual groups smoothed by adding the galaxies as Gaussians with widths $\sigma = 0.5$ mag to a finely spaced magnitude histogram, as weighted by their membership probabilities. The total luminosity function smoothed in this way is the dark solid line. The luminosity function for early type giants is the narrow solid line showing a bounded distribution at both the bright and faint ends of the total luminosity function. The spirals are shown as a dotted line and are also bounded. The early type dwarfs are shown as a solid line at the faint end of the LF. The late-type dwarfs (Sd, Sdm, Sm, and Im galaxies), shown as dotted lines, may or may not be bounded at the faint end. The total luminosity function and the early type dwarf luminosity function have been corrected for incompleteness following the prescription in Paper III. The upper and lower 1σ uncertainties in the completeness corrections are shown as dashed lines departing from the total LF below $M_{B_t} \sim -16$. The uncorrected galaxy counts for each group are shown as points with $\sqrt{N}$ error bars. The composite luminosity function for the Leo, Dorado, and NGC 1400 Groups is shown in (h), and the composite for the NGC 5044, Antlia, Fornax, and Virgo Clusters is shown in (i). These last two figures have not been corrected for incompleteness at the faint end. Ordinates for each panel span 3.0 dex.

Virgo Cluster. The shape of the dE + dS0 luminosity functions is nearly the same, as shown in Fig. 13, normalized to the counts of these galaxies brighter than $M_{B_T} = -15.0$. (The turnover in the rich group LF at $M_{B_T} = -15$ is probably due to incompleteness in the Antlia catalog.) The K–S tests show that one cannot exclude the possibility that the two samples are, in fact, drawn from the same parent distribution.

The K–S test has been used to compare the luminosity functions of each group to that of the Virgo Cluster. Results are shown in Table 4, which lists the probability (in percent) that the two distributions are drawn from the same parent distribution. [More strictly, $1 - P$ (from Table 4) is the probability that one can reject the hypothesis that the two distributions are drawn from the same parent population.] As above, the "poor" group in these tables is a composite of the Leo, Dorado, and NGC 1400 Groups; the "rich" group is a combination of the NGC 5044, Antlia, and Fornax Groups. The K–S test applied here is a comparison of the cumulative distribution of luminosities from the brightest galaxies to the magnitude limits shown. There is no way to apply completeness corrections without applying undue weight to the faintest galaxies; therefore completeness corrections have not been applied. Entries for the NGC 5044, Antlia, and composite rich groups have been omitted where the incompleteness would significantly influence the comparison. Note also that the K–S test does not account for the effects of the magnitude uncertainties. However if these are the same for all of the groups, then they should not appreciably affect the results.

The conclusions from Table 4 are (1) the luminosity functions of the luminous E, S0 and spiral galaxies are essentially the same in all seven groups, and (2) the luminosity functions of the dwarfs (dEs, dS0s and Ims) are also similar. The differences indicated between Virgo and Antlia, NGC 5044, and the combined rich group are undoubtedly due partly to the incompleteness of the surveys of the more distant groups. The difference between the Fornax and Virgo dE + dS0 luminosity function, pointed out in Ferguson & Sandage (1988; Paper I), may be real. The clear trend in the dwarf-to-giant ratio with richness shown in Figs. 1–4 does not show up strongly in the K–S test for the luminosity function over all types or even just over the early types. The reason is that significant numbers of galaxies fall in the region where dwarfs and giants overlap. Therefore, while EDGR variations still appear to exist when morphological criteria are ignored (see Fig. 4), they are at a level that is not highly significant statistically. (The morphological sorting of the data is the more powerful method.)

Our conclusion from the comparison of the raw luminosi-

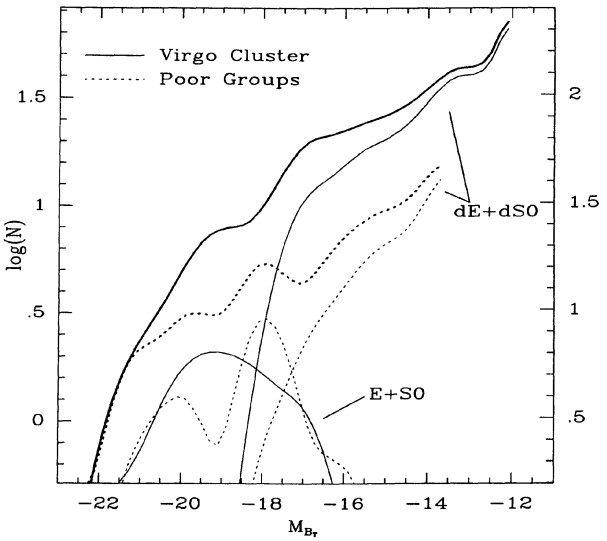

FIG. 10. Overlay of the Virgo Cluster luminosity function and the composite luminosity function for the Leo, Dorado, and NGC 1400 Groups normalized by the total number of E + S0 galaxies. The luminosity functions for the Virgo Cluster have been corrected for incompleteness; the poor-group luminosity functions have not, but the corrections are insignificant to the faintest magnitudes shown. The heavy lines show the total luminosity functions. The lighter lines show the individual luminosity functions for the E + S0 galaxies and the dE + dS0 galaxies. Note that the total luminosity functions include the contribution from late-type spirals and dwarf irregulars, which are not shown separately in this figure.

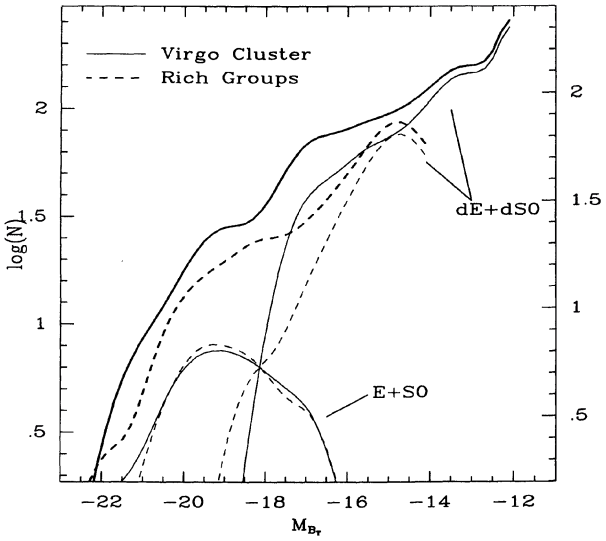

FIG. 12. Overlay of the Virgo Cluster luminosity function and the combined luminosity function of the NGC 5044, Antlia, and Fornax Groups. The latter three groups have not been corrected for incompleteness.

ty functions in this section is that *the variations in the dwarf-to-giant ratio are due to changes in the relative normalization of the giant and dwarf luminosity functions, rather than changes in their shapes.* Clearly, however, the statistical significance of this result depends on the reliability of the classification of giants and dwarfs in the luminosity interval where they overlap. However, if the EDGR variations are, in fact, real, they can be verified by reproducing Fig. 4 (which mostly avoids the region of overlap) for a larger sample of groups in future surveys.

4.2 Parametric Model Fits to the Luminosity Function

We now search for group-to-group variations in the parameters L^* and α of the Schechter (1976) form of the luminosity function. Although Figs. 9–13 show that the total

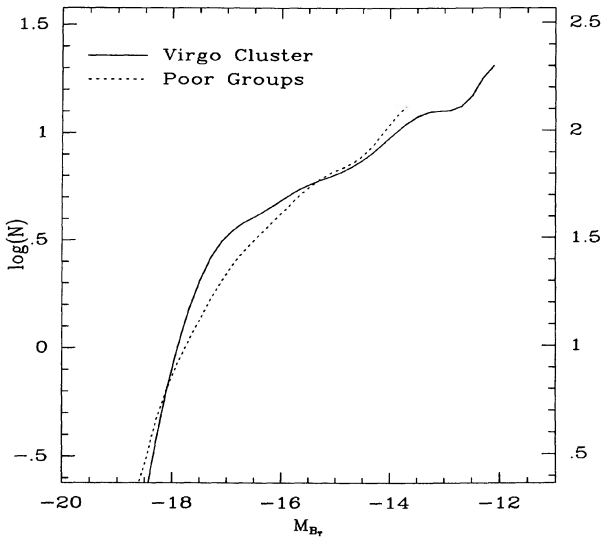

FIG. 11. Overlay of the dE + dS0 luminosity functions of the composite poor group and the Virgo Cluster. The plots are normalized by the total number of galaxies brighter than $M_{B_T} = -13.5$. The Virgo Cluster has been corrected for incompleteness at the faint end; the poor-group luminosity function has not, but the incompleteness is insignificant above $M_{B_T} = -13.5$. The similarity of shape is a crucial point here.

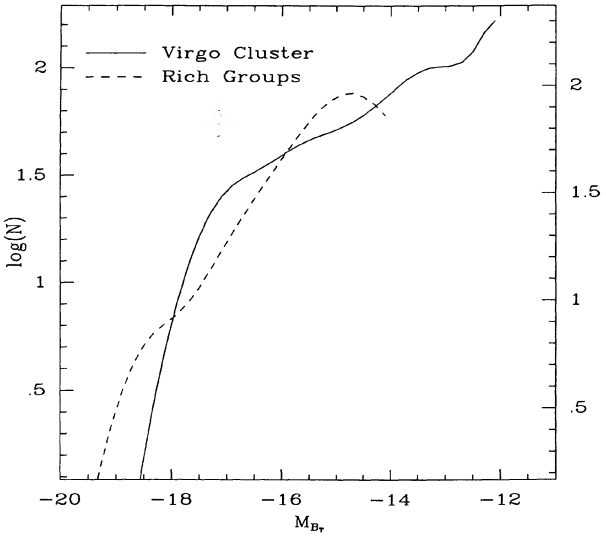

FIG. 13. Overlay of the dE + dS0 luminosity functions of the composite rich group and the Virgo Cluster. The plots are normalized by the total number of galaxies brighter than $M_{B_T} = -15$. The Virgo Cluster has been corrected for incompleteness at the faint end; the rich-group luminosity function has not, and the incompleteness starts to become significant at $M_{B_T} \sim -15.0$.

TABLE 4. K–S test results.

	All types			E+S0+dE+dE,N+dS0			E+S0
Group	-13.5	-14.5	-15.5	-13.5	-14.5	-15.5	-15.5
Leo	42.60	20.64	11.97	73.062	38.262	40.888	50.22
Dorado	50.99	37.33	30.38	72.371	76.721	80.944	78.82
NGC1400	41.89	52.86	38.56	14.300	14.781	14.830	2.09
NGC5044		0.11	0.59		1.250	0.023	53.54
Antlia			1.94			2.446	17.07
Fornax	0.17	1.85	76.47	2.769	6.949	25.070	63.54
Poor	7.06	4.62	2.31	7.200	5.241	2.335	64.89
Rich			0.56			0.050	61.83

	dE+dS0			Sd+Sdm+Sm+Im			Spirals
Group	-13.5	-14.5	-15.5	-13.5	-14.5	-15.5	-15.5
Leo	15.37	4.70	82.79	13.12	33.63	9.34	97.70
Dorado	24.99	13.17	32.58	21.61	17.77	100.00	96.71
NGC1400	76.42	99.99	87.16	89.13	65.07	100.00	94.01
NGC5044		0.10	0.72		84.02	97.53	88.86
Antlia			21.14			0.00	1.42
Fornax	0.34	0.31	0.48	64.39	21.20	46.78	83.76
Poor	88.07	73.69	96.32	18.09	22.88	20.07	49.36
Rich			10.11			0.01	4.82

function is a composite of the luminosity functions of individual Hubble types, which may have different normalizations from group to group, nevertheless, fitting the Schechter function is useful (a) for comparison with other studies of the luminosity function reported in the literature, and (b) to characterize possible deviations from this "universal" function for our sample.

Schechter functions have been fit to the composite poor group and to the individual richer groups. Fitting was performed on the unbinned data using a maximum likelihood technique similar to that described by Malumuth & Kriss (1986) and Oegerle *et al.* (1986). For our sample, the likelihood of obtaining the N absolute magnitudes M_i drawn at random from a Schechter function is given by

$$L = \prod_{i=1}^{N} \frac{w_i \phi(M_i) C(M_i) dM}{\int_{-\infty}^{M_{\rm lim}} \phi(M) C(M) dM}, \qquad (2)$$

where $\phi(M)$ is the Schechter function of Eq. (1), w_i are the membership weightings described in Sec. 22, $M_{\rm lim}$ is the limiting magnitude used for the fit, and $C(M)$ are related to the completeness corrections by Eq. (4) of Paper III by $C(M) = 1/F(M)$. We maximize the likelihood by minimizing the quantity $S = -2 \ln L$,

$$S = 2N \ln\left(\int_{-\infty}^{M_{\rm lim}} \phi(M) C(M) dM\right) - 2 \ln[w_i \phi(M_i) C(M_i)]. \qquad (3)$$

The integral was evaluated numerically and parameter space was searched for the best fit using the simplex algorithm (Nelder & Mead 1965). The intervals in S about the minimum are directly related to confidence intervals for the parameters α and M^* (Avni 1976; Cash 1979). In particular, S is distributed about the minimum approximately as χ^2_ν where ν is the number of "interesting parameters" for which confidence intervals are desired (Avni 1976). The resulting best-fit functions and confidence intervals in the Schechter parameters are shown in Figs. 14–16. The values of the parameters for the best fits are shown in Table 5.

Consider first the total luminosity functions shown in Fig. 14. While the Schechter parameters for the total luminosity function of the Antlia and Fornax Clusters differ from those of the Virgo Cluster at about the 3σ level (α for Virgo is less negative than for the others), there is no obvious trend in α or M^* with richness. The parameters for the NGC 5044 and the poor groups are consistent to within 3σ with those for Virgo. The value of M^* is not well constrained for any of the groups other than Fornax and Virgo.

Figure 14 shows that the Schechter function is not a particularly good fit to the Antlia and NGC 5044 groups using all galaxy types. This is confirmed by a K–S test made by comparing the cumulative distribution of the *observed* magnitudes to the cumulative distribution predicted by the best-fit Schechter function. The results of the K–S tests are listed in the sixth column of Table 5 (top section), modified to account for the fact the magnitudes are not estimated to arbitrary precision (see below). The listed number is the percent probability that the observed distribution is drawn from the adopted Schechter distribution. Except for the Leo, Dorado, and NGC 1400 Groups individually, the K–S test shows that the observed distribution of magnitudes for any of the groups is unlikely to have been drawn at random from a Schechter function. The most significant deviation from the Schechter function is for the Virgo Cluster, where the larger number of galaxies make the test more sensitive.

But results from the K–S test should not be taken at face value because they do not take into account the uncertainties in the magnitudes, completeness corrections, membership classifications, or the finite resolution of the magnitude determinations. To investigate the effect of magnitude uncer-

TABLE 5. Best-fitting luminosity-function parameters.

Group Name	Limiting M_{B_T}	N	α	M^*	K-S prob. %	χ^2	ν
All Types (Schechter fit)							
Leo	-12.5	28.9	-1.36	-22.84	47.6	13.6	24
Dorado	-12.5	36.9	-1.34	-22.32	32.0	10.1	24
NGC1400	-13.0	63.0	-1.44	-21.27	17.7	18.0	23
Poor	-13.0	120.7	-1.39	-22.17	5.9	16.8	23
NGC5044	-14.0	108.6	-1.56	-23.20	1.0	54.6	21
Antlia	-14.5	238.5	-1.55	-22.54	0.3	53.9	20
Fornax	-12.5	331.5	-1.38	-21.47	0.2	30.9	24
Virgo	-12.5	1068.1	-1.29	-21.23	0.1	51.9	24
dE + dS0 Galaxies (Schechter fit)							
Leo	-12.5	13.6	-1.65	-16.19	76.9	4.0	24
Dorado	-12.5	15.8	-1.51	-16.61	73.8	3.4	24
NGC1400	-13.0	42.1	-1.62	-18.69	54.8	7.5	23
Poor	-13.0	64.4	-1.65	-18.30	64.9	5.8	23
Ngc5044	-14.0	64.7	-1.98	-20.86	53.7	32.2	21
Antlia	-14.5	141.5	-2.09	-20.68	68.7	65.1	20
Fornax	-12.5	223.9	-1.14	-16.35	30.5	21.2	24
Virgo	-12.5	733.8	-1.28	-17.42	0.0	63.3	24
E + S0 + dE + dS0 Galaxies (Schechter fit)							
Leo	-12.5	18.1	-1.47	-23.77	87.3	7.6	24
Dorado	-12.5	22.4	-1.47	-23.07	72.1	7.9	24
NGC1400	-13.0	55.7	-1.50	-21.66	18.4	16.6	23
Poor	-13.0	89.1	-1.48	-22.61	33.6	15.6	23
NGC5044	-14.0	83.8	-1.68	-23.58	1.7	42.5	21
Antlia	-14.5	179.7	-1.75	-24.56	1.8	55.1	20
Fornax	-12.5	264.9	-1.46	-21.77	0.2	31.7	24
Virgo	-12.5	813.9	-1.42	-21.73	0.02	49.5	24

tainties, we constructed artificial datasets and compared them to Schechter functions using the same techniques we used for the real data. We first produced 1000 datasets with no magnitude errors and applied the K–S test comparing the simulated data to the true distribution. The K–S test gives the probability of observing a maximum difference D between the cumulative distributions greater than the observed difference if the dataset is drawn at random from the true distribution. The results are as expected when errors were assumed to be zero, i.e., 99% of the time the K–S test returns a probability greater than 1%. Next we added random errors to the magnitudes distributed as a Gaussian with width $\sigma = 0.5$ mag, and compared the simulated distribution to the theoretical distribution. The K–S test returned a probability greater than 1% only 79% of the time, indicating that the K–S test is too stringent when magnitude errors are involved. Finally, we used the maximum-likelihood technique to find the best fit Schechter function for the simulated data and used the K–S test to compare the fit to the data. In this case, 99.6% of the time, the K–S test returned a probability greater than 1%. Thus, if the magnitude errors are truly random, a Schechter function will be a good fit to the data if the true distribution is, in fact, Schechter, but will generally have different values of α and M^* than the true distribution. The important corollary is that if the magnitude errors are truly random and the K–S test comparing the observed distribution to the best-fit Schechter function does return a low probability, then the Schechter function is probably the wrong model for the composite (i.e., non-type-specific) luminosity function.

The other sources of error mentioned in Sec. *2.2* are to model in the same way as above, making it impossible to entirely rule out the Schechter function based on K–S tests to our data. To test the effect of the uncertain members (class 3), we have eliminated them from the dataset and fit Schechter functions as before. The result is that most of the distributions are flatter (most of the uncertain members are faint), and the Schechter function is a better fit. However, it is still rejected by the K–S test with a high probability in the Virgo Cluster and NGC 5044 Group.

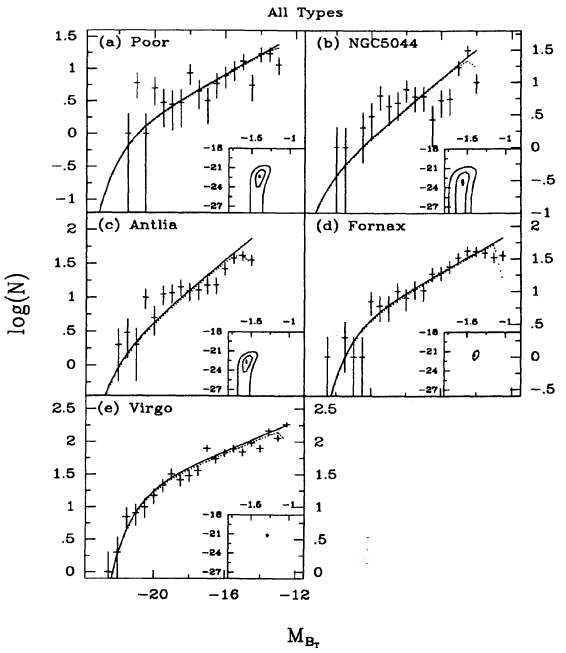

FIG. 14. Results of fitting a Schechter (1976) luminosity function to the observed magnitude distributions. The logarithm of the number of galaxies in half-magnitude bins is shown plotted against absolute magnitude for (a) a composite "poor" group made up of the Leo, Dorado, and NGC 1400 Groups, (b) the NGC 5044 Group, (c) the Antlia Group, (d) the Fornax Cluster, and (e) the Virgo Cluster with data taken from BST85. The best-fit Schechter function is shown as a solid line without the completeness correction, and as a dotted line with the completeness correction applied. The insets show the confidence intervals on the α and M^* parameters. The outer contour is the 99.9% confidence interval, the next contour in is the 68% confidence interval, and the central contour shows essentially the location of the best fit. Data are binned for display purposes only; all fitting was carried out on the unbinned distributions.

Finally, the magnitudes in our catalogs are not drawn at random but have been estimated to the nearest 0.1 mag (i.e., binned in 0.1 mag bins). This tends to lower the probability returned by the K–S test by an amount that depends both on the number of galaxies and the luminosity function. We have accounted for this effect by comparing the K–S test results for simulated datasets binned at 0.1 mag to those of the same dataset binned at 0.0001 mag (i.e., essentially unbinned). For example, for a simulated dataset with the Virgo Cluster luminosity function and 1068 galaxies, the K–S test returns a probability for the binned data that is 0.6 times the probability for the unbinned data. We have computed correction factors for the parameters listed in Table 5, and have applied them to the raw K–S test results to produce the numbers listed in the sixth column. Correction factors varied from 1.0 for the poor groups, to 0.5 for the Virgo Cluster. Note that the Virgo Cluster will also be much more sensitive to small systematic errors in the magnitudes than the groups with fewer galaxies.

As an alternate statistical test, we have binned the galaxies in 0.5 mag bins, and compared the best-fit Schechter function to the observed distribution via the χ^2 test. The resulting values of χ^2 are shown in column 7 of Table 5, followed by the number of degrees of freedom.

Examination of Fig. 14 indicates that the problem with the Schechter function is as follows: The slope of the Schechter function is mostly constrained by the faint dwarfs, which have the greatest numbers and therefore the smallest statistical errors. However, extrapolation of this slope to bright magnitudes tends to undershoot the giants (in Antlia and NGC 5044 in particular). For most of the groups in Fig. 14, the data points show an observed $\phi(M)$ that is almost flat in the interval from $M_{B_T} = -20$ to -16, followed by a more rapid rise at fainter magnitudes. Such a flattening at intermediate luminosities might account for the difference between the canonical $\alpha = -1.25$ slope in clusters and the flatter $\alpha \sim -1$ for loose groups and the field (Turner & Gott 1976; Kirshner *et al.* 1979; Davis & Huchra 1982). Note that most studies of the luminosity function have included only galaxies *brighter* than $M_{B_T} = -16$. At this luminosity cutoff, rich clusters are already dominated by dEs, which have a steeply rising faint end, while poorer groups and the field still have significant contributions from giants, with their nearly Gaussian luminosity distributions. Hence the combination of two forms for $\phi(M)$ with different normalizations will produce the apparent difference in α for the "total" function. To test this idea, we have fit the total luminosity functions for the groups in our sample down to a magnitude cutoff of $M_{B_T} = -16$ with results shown in Table 6. The best-fit values of α are indeed close to 1.0 for the poor groups and are steeper for the richer ones. Because the already small samples from the poor groups have been pared down even further by this magnitude cutoff, the formal significance of the difference between α for the poor groups and the Virgo Cluster is marginal, but it does suggest that the variation in α from previous surveys can be understood as an artifact of the incorrect parametrization of the composite luminosity distribution as a Schechter function, rather than a sum of distinct, type-dependent, luminosity functions.

Figure 15 shows the luminosity function for just the dwarf ellipticals and dS0s, compared to the best-fit Schechter function. With the possible exception of Fornax, all of the groups show distributions that are still rising steeply at the faint end. The K–S tests confirm the visual impression that the Schechter function is a much better fit to these distributions (but is still formally rejected for Virgo). The slope α is significantly steeper for the NGC 5044 and Antlia Groups. Since these are the two most distant groups, it is likely that this is in part due to contamination by faint background and foreground galaxies. The slopes are somewhat flatter when the membership class 3 galaxies are omitted, but still appear to be steeper than for Virgo, Fornax, and the poor groups.

The combined luminosity function for the early type giant E and S0 galaxies and the dwarf dE and dS0 galaxies is

TABLE 6. Best-fitting Schechter functions brighter than $M_{B_T} = -16$.

Group	N	α	M^*
Leo	10.5	-1.05	-21.80
Dorado	14.5	-1.00	-21.32
NGC1400	22.3	-1.19	-20.41
Poor	47.3	-1.16	-21.42
NGC5044	49.1	-1.15	-21.11
Antlia	123.8	-1.24	-21.23
Fornax	88.5	-1.41	-21.93
Virgo	347.9	-1.34	-21.48

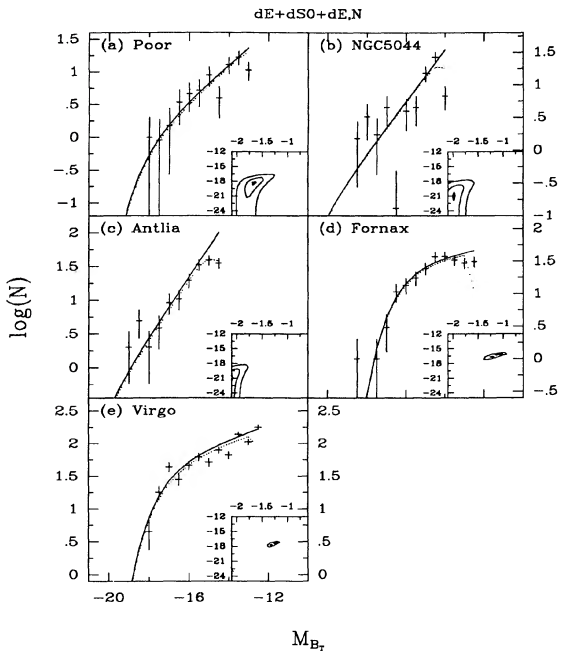

FIG. 15. Schechter function fits to the luminosity functions of early type dwarf galaxies in each group, the dwarfs being chosen by morphology alone.

shown in Fig. 16. Once again, the Schechter function is not a good fit to the total data [a fact that was initially pointed out by Sandage *et al.* (1985) for the Virgo Cluster].

We now consider the case suggested several times above where the "total" function is a combination of a Gaussian luminosity function for the E and S0 galaxies,

$$\phi(M) \sim \exp[-(M-\mu)^2/2\sigma^2],$$

and a Schechter function for the dwarfs. The results are given in Table 7 and are plotted in Fig. 17, together with the best-fit Schechter function for the dE + dS0 galaxies and the combined dE + dS0 + E + S0 distribution. Note that the intrinsic dispersion of the Gaussian LF will be smaller than that shown in Table 7 ($\sigma^2_{\text{true}} \approx \sigma^2_{\text{obs}} - \sigma^2_{\text{errors}}$) because the luminosity functions shown are convolved with the magnitude errors. The Gaussian distributions in the Fornax Cluster and the poor groups are skewed toward faint magnitudes (and hence have fainter μ in Table 7) by the presence of a population of compact ellipticals (included in the fits with low weight) whose membership is uncertain. It is perhaps more likely that most of these are background galaxies, and indeed spectra from many of the candidates in Paper II, Table 13 have so far confirmed only one candidate as a member (Kimble *et al.* 1990). (The confirmation rate is higher for the list of M32-like objects in the Virgo Cluster, however, due possibly to different selection criteria for these candidates in the Virgo Cluster catalog.) In Fig. 18 we show the distributions when only likely cluster members are included. Note that the variations in the EDGR and the trends with richness discussed in the previous sections are still significant even if the compact ellipticals are not, in fact, cluster members, as can be verified by comparison of the columns listing N in Tables 5 and 7. The dwarf-to-giant ratio has changed slightly but still varies significantly from the poor groups to Virgo. The best-fit parameters are shown in Table 7. Comparing the curves in Fig. 18, it is clear that the combination of a Gaussian for the giants plus a Schechter function for the dwarfs is a better fit to the data than a single Schechter function, and that the relative normalization of

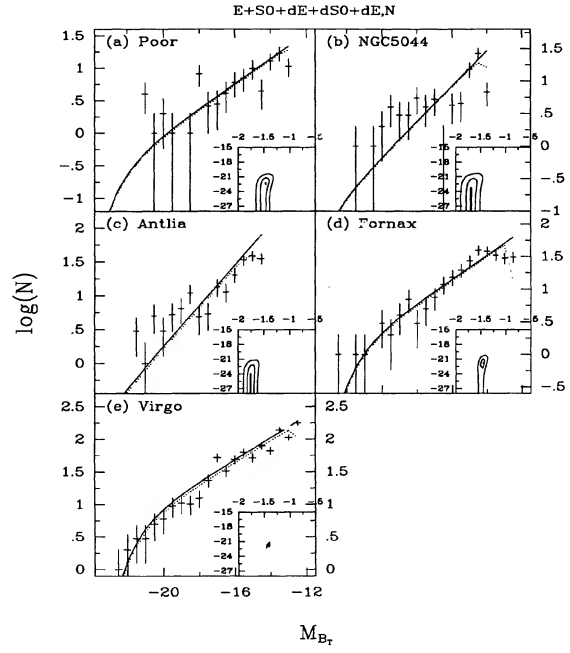

FIG. 16. Schechter function fits to the combined luminosity functions of E, S0, dE, and dS0 galaxies in each group.

TABLE 7. Best-fitting Gaussian luminosity functions.

Group Name	Limiting M_{B_T}	N	σ	μ	K-S prob. %
E + S0 Galaxies (membership classes 1, 2, and 3)					
Leo	-12.5	5.0	2.80	-16.96	15.1
Dorado	-12.5	7.1	2.38	-16.94	39.1
NGC1400	-13.0	13.6	1.67	-17.09	3.7
Poor	-13.0	25.7	2.18	-16.98	2.6
NGC5044	-14.0	19.6	1.45	-18.34	36.4
Antlia	-14.5	41.2	1.60	-18.43	8.6
Fornax	-12.5	42.2	2.42	-16.22	0.08
Virgo	-12.5	78.7	1.75	-18.31	33.7
E + S0 galaxies (membership classes 1 + 2)					
Leo	-12.5	3.5	0.41	-20.38	97.9
Dorado	-12.5	5.3	1.59	-19.11	91.1
Ngc1400	-13.0	12.1	1.21	-17.98	44.0
Poor	-13.0	20.9	1.52	-18.63	51.7
NGC5044	-14.0	18.8	1.19	-18.71	90.5
Antlia	-14.5	37.4	1.38	-18.95	80.0
Fornax	-12.5	34.2	1.77	-18.21	73.6
Virgo	-12.5	74.5	1.48	-18.81	73.4

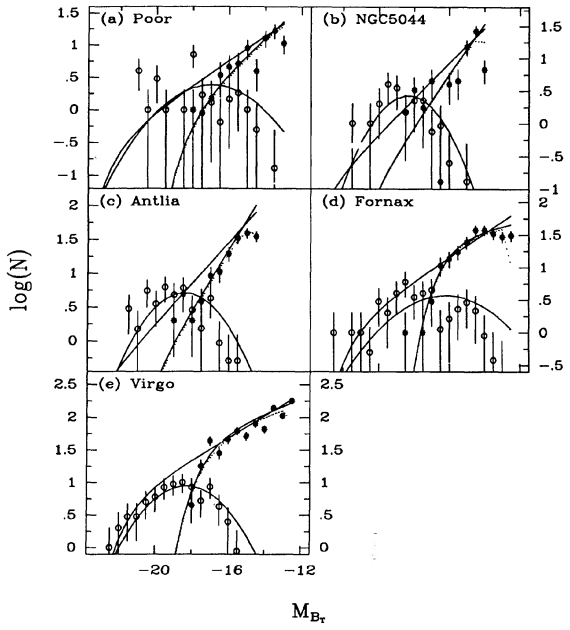

FIG. 17. Composite luminosity function of early type galaxies. The E and S0 galaxies are shown as open circles with the best-fit Gaussian superimposed as a solid curve. The dE and dS0 galaxies are shown as asterisks, with the best-fit Schechter function superimposed as a solid curve. The Schechter function with the incompleteness correction is shown as a dotted line. Also shown is the best-fit Schechter function to the combined distribution from Fig. 16.

the two functions varies from group to group.

A physical basis for such a separation of the dwarf and giant luminosity functions was put forward by Schaeffer & Silk (1988). In their model, the separation between dwarfs and giants is due to the onset of supernova driven galactic winds at a critical virial velocity of ~ 100 km s^{-1}. The faint end slope of the dwarfs is determined by the initial fluctuation spectrum at the time of galaxy formation. The theoretical slope in their model is in reasonable agreement with the observed slopes for the dwarf galaxy luminosity functions in our sample fit to faint magnitude limits (Leo, Dorado, NGC 1400, Fornax, and Virgo) if the spectrum is a power law $P(k) \sim k^n$ with $n \sim 1$. (Note that $n \sim 2.4$ would be required in this model if the field galaxy slope $\alpha \sim -1.1$ were to extend to fainter magnitudes.)

The Schaeffer and Silk model also predicts that the luminous galaxies should be more spatially correlated by a factor of 2–4 than the dwarf galaxies, and therefore that the relative normalizations of the dwarf and giant luminosity functions should vary from place to place. Such a variation has been detected in our sample, but it is not clear how to interpret our finding that the giant galaxy content is *higher* in the poor groups (or conversely, that the dwarfs are overabundant relative to the giants in the rich clusters compared to the poor groups). Note that Schaeffer and Silk's model predicts that the field galaxy luminosity function should be *steeper* in the field than in clusters, even when fit down to $M_{B_T} = -16$, contrary to what is observed both in our sample and in studies of $\phi(M)$ for field galaxies.

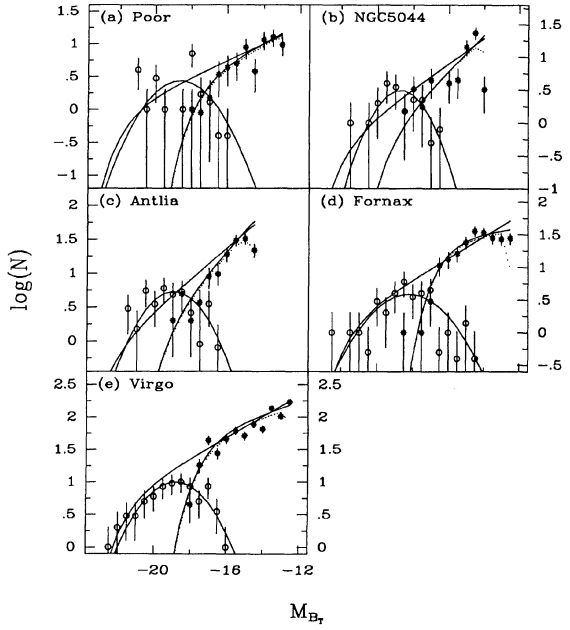

FIG. 18. Same as Fig. 17 with uncertain members (membership class 3 galaxies) removed.

5. CONCLUSIONS

The comparison of the galaxy populations in the nearby groups studied here permit the following conclusions.

(1) Significant differences exist in the dwarf-to-giant ratio for early type galaxies from group to group. The Virgo Cluster and the rich groups have higher dwarf-to-giant ratios than the poorest groups.

(2) The dwarf-to-giant ratio for early type galaxies increases monotonically with richness of the groups.

(3) This correlation is probably *not* due to variations in the mean densities or the spatial sampling of the groups or the morphological classification of the galaxies, or to uncertainties in the magnitude estimates or completeness limits of the catalogs, but, observationally is related only to the richness of the aggregate.

(4) There is an indication that the dwarf-to-giant ratio is correlated with group velocity dispersion.

(5) There are no radial gradients in the dwarf-to-giant ratio for the Antlia, Fornax, and Virgo Clusters in our data, showing that mass segregation has probably not occurred, contrary to the expectation from West & Richstone (1988) if the clusters have undergone violent relaxation.

(6) No systematic trends with richness are apparent in the L^* and α parameters of the Schechter function, but the Schechter function is probably not the correct model for the composite "total" luminosity function of the early type galaxies or for the luminosity function of the giant (E, S0, and Spiral) galaxies alone. A combination of a Gaussian for the giants and a Schechter function for the dwarfs produces a better fit to the data.

(7) The variations in the dwarf-to-giant ratio and the value of α for the total function between small groups and clusters are due to changes in the relative normalization of the giant and dwarf luminosity functions, rather than changes in their shapes. Such variations provide an explanation for the apparent difference in the faint end slope of $\alpha \sim -1$ for field samples and $\alpha \sim -1.3$ for cluster samples. The difference is

not real but is an artifact of incorrectly discussing the total $\phi(M)$ using a Schechter function rather than discussing type-specific luminosity functions with different normalizations for their sum.

If the variation in the relative populations of dwarfs and giants is real, then it provides a constraint on theories of the evolution of dwarf galaxies. Mergers of dwarfs and giants may play an important role in depleting the dwarf galaxy population in the low-velocity-dispersion groups. Alternatively, tidal encounters between galaxies in richer groups and clusters may produce debris that collapses into dwarf galaxies. In either case, the variation in EDGR between poor groups and rich clusters offers a challenge to hierarchical formation models in which rich clusters formed from the merging of small groups.

It is a pleasure to thank Gustav Tammann and Bruno Binggeli for key ideas leading to this work, including the suggestion that the total luminosity function be treated as a sum of different type-specific luminosity functions. We are also indebted to Binggeli for providing the galaxy counts from the 10 Mpc sample used in Figs. 1–3. We are grateful to Jerry Kriss for useful discussions on fitting luminosity functions. H. C. F. is grateful for the support of the NASA Graduate Researchers Program and the Hopkins Ultraviolet Telescope Project.

REFERENCES

Abell, G. O. 1975, in Galaxies in the Universe (Stars and Stellar Systems, Vol. 9), edited by A. Sandage, M. Sandage, and J. Kristian (University of Chicago Press, Chicago), p. 601
Avni, Y. 1976, ApJ, 210, 642
Binggeli, B. 1987, in Nearly Normal Galaxies, edited by S. Faber (Springer, New York), p. 195
Binggeli, B. 1988, in Large-Scale Structure and Motions in the Universe, edited by M. Mezzetti, G. Giuricin, F. Mardirossian, and M. Ramella (Kluwer, Dordrecht)
Binggeli, B., Sandage, A., and Tammann, G. A. 1985, AJ, 90, 1681 (BST85)
Binggeli, B., Sandage, A., and Tammann, G. A. 1988, ARA&A, 26, 509
Binggeli, B., Tarenghi, M., and Sandage, A. 1990, A&A, 228, 42
Binney, J., and Tremaine, S. 1987, Galactic Dynamics (Princeton University, Princeton), p. 611
Bothun, G., Beers, T. C., Mould, J. R., and Huchra, J. P. 1986, ApJ, 308, 510
Cash, W. 1979, ApJ, 228, 939
Choloniewski, J. 1986, MNRAS, 223, 1
Davis, M., and Djorgovski, S. 1985, ApJ, 299, 15
Davis, M., and Huchra, J. 1982, ApJ, 254, 437
Dekel, A., and Silk, J. 1986, ApJ, 303, 39
Dressler, A. 1978, ApJ, 223, 765
Dressler, A. 1980, ApJ, 236, 361
Eder, J., Schombert, J. M., Dekel, A., and Oemler, A. 1989, ApJ, 340, 29
Ellis, R. 1983, in The Origin and Evolution of Galaxies, edited by B. J. T. Jones and J. E. Jones (Reidel, Dordrecht), p. 255
Felten, J. E. 1977, AJ, 82, 861
Ferguson, H. C., and Sandage, A. 1988, AJ, 96, 1520 (Paper I)
Ferguson, H. C. 1989, AJ, 98, 367 (Paper II)
Ferguson, H. C., and Sandage, A. 1990, AJ, 100, 1 (Paper III)
Giovanelli, R., Haynes, M. P., and Chincarini, G. L. 1986, ApJ, 300, 77
Hubble, E., and Humason, M. L. 1931, ApJ, 74, 43
Kimble, R. A., Davidsen, A. F., and Ferguson, H. C. 1990, in preparation
Kirshner, R. P., Oemler, Jr., A., and Schechter, P. L. 1979, AJ, 84, 951
Kraan-Korteweg, R. C., and Binggeli, B. 1990, in preparation
Kraan-Korteweg, R. C., Sandage, A., and Tammann, G. A. 1984, ApJ, 283, 24
Malumuth, E. M., and Kriss, G. A. 1986, ApJ, 308, 10
Nelder, J. A., and Mead, R. 1965, Comput. J., 7, 308
Oemler, A. 1974, ApJ, 194, 1
Oegerle, W. R., Hoessel, J. G., and Ernst, R. M. 1986, AJ, 91, 697
Phillipps, S., and Disney, M. 1986, MNRAS, 221, 1039
Phillipps, S., and Shanks, T. 1987, MNRAS, 229, 621
Postman, M., and Geller, M. J. 1984, ApJ, 281, 95
Salzer, J. J., Hanson, M. M., and Gavazzi, G. 1990, ApJ, 353, 39
Sandage, A., Binggeli, B., and Tammann, G. A. 1985, AJ, 90, 1759 (SBT85)
Schaeffer, R., and Silk, J. 1988, A&A, 203, 273
Schechter, P. 1976, ApJ, 203, 297
Shanks, T., Stevenson, P. R. F., Fong, R., and MacGillivray, H. T. 1984, MNRAS, 206, 767
Sharp, N. A., Jones, B. J. T., and Jones, J. E. 1978, MNRAS, 185, 457
Spinrad, H. 1986, PASP, 98, 269
Spinrad, H., and Djorgovski, S. 1987, in Observational Cosmology, IAU Symposium No. 124, edited by A. Hewitt, G. Burbidge, and L. -Z. Fang (Reidel, Dordrecht), p. 129
Tammann, G. A., Yahil, A., and Sandage, A. 1979, ApJ, 234, 775
Thompson, L. A., and Gregory, S. A. 1980, ApJ, 242, 1
Thuan, T. X., Gott III, J. R., and Schneider, S. E. 1987, ApJL, 315, L93
Tully, R. B. 1988, AJ, 96, 73
Turner, E. L., and Gott, J. R. 1976, ApJ, 209, 6
Tyson, J. A. 1988, AJ, 96, 1
West, M. J., and Richstone, D. O. 1988, ApJ, 335, 532
White, S. D. M., Tully, B., and Davis, M. 1988, ApJL, 333, L45
White, S. D. M., Davis, M., Efstathiou, G., and Frenk, C. S. 1987, Nat, 330, 451
Yee, H. K. D., and Green, R. F. 1987, ApJ, 319, 28
Yoshii, Y., and Takahara, F. 1988, ApJ, 326, 1